actuators

MDPI

Article

A Large Force Haptic Interface with Modular Linear Actuators

Yeongtae Jung [1,2,*] and Joao Ramos [3,4]

[1] Department of Mechanical System Engineering, Jeonbuk National University, Jeonju 54896, Republic of Korea
[2] Advanced Transportation Machinery Research Center, Jeonbuk National University, Jeonju 54896, Republic of Korea
[3] Department of Mechanical Science and Engineering, University of Illinois at Urbana-Champaign, Urbana, IL 61801, USA; jlramos@illinois.edu
[4] Department of Electrical and Computer Engineering, University of Illinois at Urbana-Champaign, Urbana, IL 61801, USA
* Correspondence: ytjung@jbnu.ac.kr

Abstract: This paper presents a haptic interface with modular linear actuators that addresses the limitations of conventional devices based on rotary joints. The proposed haptic interface is composed of parallel linear actuators that provide high backdrivability and small inertia. The performance of the haptic interface is compared to those of conventional mechanisms in terms of force capability, reflected inertia, and structural stiffness. High stiffness, large range of motion, and high force capability, which are in trade-off relationships in traditional haptic interfaces, are achieved. The device can apply up to 83 N continuously, i.e., three-fold more than most haptic devices. The theoretical minimum haptic force density and stiffness of the proposed mechanism are 1.3 to 1.9 and 37 times those of the conventional mechanisms under similar conditions, respectively. The system is scalable because the structural stiffness depends on only the timing belt stiffness, whereas that of conventional haptic interfaces is inversely proportional to the cube of the structural length. The modular actuator enables changes in the degrees of freedom (DOFs) for different applications. The proposed haptic interface was tested through an interaction experiment in a virtual environment with virtual walls.

Keywords: haptic interfaces; parallel robots; human–robot interaction

Citation: Jung, Y.; Ramos, J. A Large Force Haptic Interface with Modular Linear Actuators. *Actuators* **2023**, *12*, 293. https://doi.org/10.3390/act12070293

Academic Editors: Qing Guo and Wei Yang

Received: 30 June 2023
Revised: 12 July 2023
Accepted: 13 July 2023
Published: 18 July 2023

1. Introduction

A haptic interface allows for physical interaction between a user and a virtual environment. The hardware and controller determine the transparency and stability in rendering an environment. Although advanced control algorithms can enhance the performance of haptic interfaces [1–4], transparency and stability conflict in the sense of control, as introduced in [5]. Therefore, the fundamental limitation of a haptic system is determined by the physical system of the device, including the actuator bandwidth, structural stiffness, friction, inertia, and range of motion (ROM). Haptic interface hardware design always introduces trade-offs between these parameters. A large ROM requires long linkages, which are associated with low structural stiffness or large reflected inertia from the linkage mass. A large force capability requires high gearing ratios, which are associated with high friction and reflected inertia [6]. These trade-off relationships are dominated by the actuators, transmissions, and sensors, and depend on the mechanism that combines the components of a haptic interface.

Serial mechanisms with rotational actuators, which are widely used in robotic arms and exoskeletons, can be considered as the mechanism of a haptic interface [7–9]. This mechanism is simple and allows for a large ROM because interference between linkages can be prevented by an appropriate design. However, cumulative linkage deformation (principally bending) negatively affects the displayable stiffness at the end-effector. Thus, large inertia of the linkage is required to ensure high stiffness. While it is necessary

to increase the gear ratio of the actuator to handle the large inertia, this reduces the backdrivability of the haptic interface.

For this reason, most commercial haptic interfaces use parallel linkage-based mechanisms such as the delta mechanism [10] or four-bar linkages [11–13]. Parallel linkages enhance structural stiffness of the system while limiting ROM because of their structural complexity. The commercial haptic interfaces cited above show force capabilities of less than 20 N because high reduction ratio gears are avoided to ensure high transparency. The 3-DOF Orthogonal Tripteron mechanism introduced in [14] allows fully decoupled motion of all three axes; thus, the kinematics and dynamics are simple. However, the stiffness is limited because of the bending of linkages. Interference between rotational linkages and the user becomes problematic when the system is upsized. The actuators are high-speed small-torque motors with gear reductions.

Admittance control with force feedback could be an option for reducing the effects of friction imparted by gearing. This yields lightweight and high-force systems with small actuators. However, the haptic feedback bandwidth and stability are limited by the sensing rate and sensor noise. A high gear ratio and the resulting reflected inertia limit the bandwidth at high frequency [15]. Perret et al. [16] used a tendon-driven haptic interface to enable room-size ROM. However, the stiffness was limited by the long tendon, and the tendons could interfere with the user. Brake-and-clutch systems can deliver high force with backdrivability [17,18], but can only render resistive environments. A hybrid actuation system with a clutch and an active actuator could render a very high stiffness while capable of displaying a small-force active environment when the clutch is not activated. However, only infinite stiffness environments could be delivered, and would not allow modulation of perceived contact compliance when the clutch is activated [19].

Certain non-commercialized haptic interfaces have targeted high force capabilities, ROMs, and high backdrivability [15,20,21]. One hybrid actuation mechanism separated high- and low-frequency force generation using different sizes of actuators for the base part and distal side [15]. However, the system was highly complex, and it required control efforts in contact with high stiffness virtual objects. Lee et al. used parallel four-bar linkages that can provide a large ROM and high force capability and stiffness [20]. However, gears with high reduction ratio were used to enhance the force capability, which was associated with large reflected inertia of the actuator at the end-effector side along with friction. Thus, it had a high overshoot and long settling time. Barnaby et al. developed a haptic interface with backdrivable actuators, timing belt reductions, and a four-bar linkage mechanism [21]. While the system showed high backdrivabilty, the force was as low as those of commercial haptic interfaces.

All of the above-mentioned haptic interfaces used rotational actuation mechanisms. This introduces *bending* deflection of the linkages, which is a dominant deflection of the structure. Although the actuators provide high stiffness, the low structural stiffness limits the displayable stiffness at the extremity of the linkages.

We aim to develop a large force haptic interface for the teleoperation system shown in Figure 1 [22–24]. The system utilizes the user's skills to explore the dynamic balancing and manipulation of the teleoperated robot. The user and robot are synchronized, with human motion used as the reference; the user receives feedback through a human–machine interface (HMI). The kinematic and dynamic differences between human and robot reduced models, such as a linear inverted pendulum and wheeled inverted pendulum model, are used for control. With the synchronized teleoperation system, the user can achieve dynamic manipulations such as pushing a heavy object by leaning against it, thereby leveraging body weight and inertia. A human can generate almost 140 N of push force under practical conditions and even more under certain circumstances [25]. It is necessary to provide such a large force to the user's hand to make the human and robot dynamically similar; this significantly affects the dynamics of both the human and the robot. To leverage the full balancing and manipulation capacities of a human, the ROM should

cover roughly a human quadrant. This is difficult to achieve with existing haptic interfaces without scarifying stiffness, considering the limitations of rotational mechanisms.

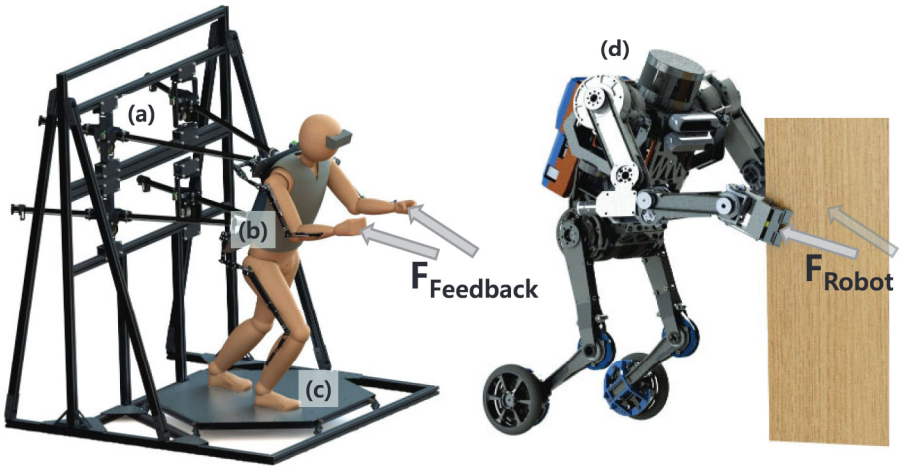

Figure 1. Dynamic teleoperation system with human–machine interface (HMI): (**a**) backdrivable linear actuators, (**b**) high-speed motion capture system, (**c**) force plate, and (**d**) teleoperated robot.

In this paper, we propose a novel haptic interface based on modular linear actuators that can provide a large force, large ROM, high mechanical backdrivability, small reflected inertia, and high structural stiffness (Figure 2) as a part of the human–robot interaction system. The mechanism is compared to those of conventional serial and parallel mechanisms in terms of the available force over reflected inertia. The proposed mechanism is scalable because high structural stiffness is ensured by the linear actuator-based mechanism regardless of the ROM; in addition, the reflected inertia is small. The actuator ensures high force capability and backdrivability because of the timing belt-based reduction. A gimbal handle that connects two modular linear actuators and ensures zero residual torque is introduced as an example for the proposed haptic interface design. Considering the parallel linear mechanism, the DOFs can be varied by adding additional modular linear actuators and modifying the handle design without being significantly constrained by structural stiffness or the inertia of the system.

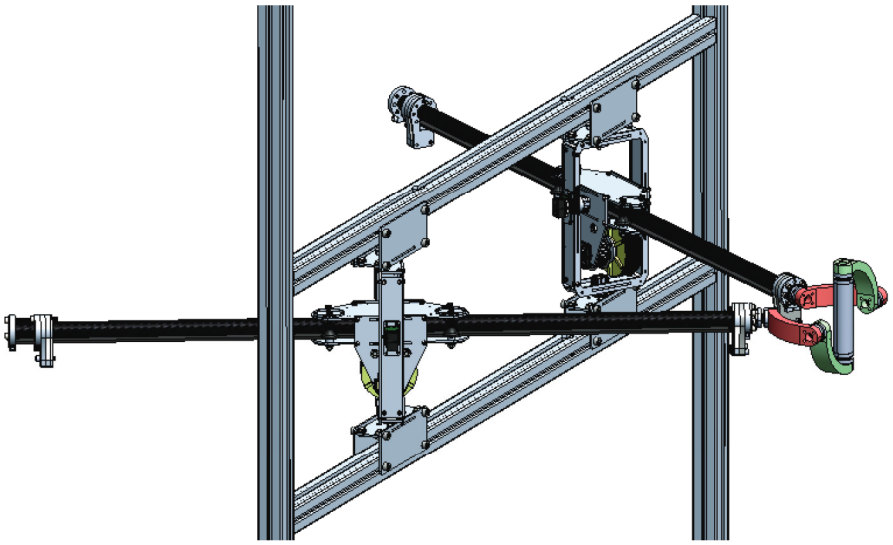

(**a**)

Figure 2. *Cont.*

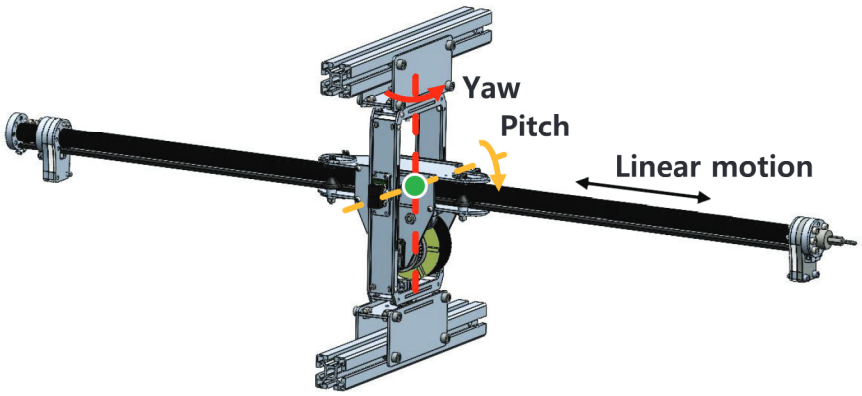

(**b**)

Figure 2. The proposed planar linear haptic interface with modular actuators: (**a**) haptic interface and (**b**) modular actuator.

The remainder of this article is organized as follows. In Section 2, the design of our haptic interface with linear actuators is introduced and analyzed in comparison to conventional rotational mechanisms. The performance of the backdrivable modular linear actuator is addressed in Section 3. The results of experiments with a virtual object are presented in Section 4 along with a discussion. Finally, Section 5 concludes the article.

2. Mechanism Design and Analysis

2.1. Design

The main limitations of previous haptic systems are induced by friction and inertia from gearing [6] as well as by low stiffness caused by bending of the linkages. We propose a haptic interface with modular linear actuators that can overcome these limitations (Figure 3a). The modular linear actuators proposed in [22] are connected in parallel to the end-effector. The actuator has high-torque low-inertia motors and a timing belt-based reduction system that together enable a high force capability of up to 100 N and backdrivable actuation with small friction. Thus, the haptic interface is very transparent. The actuator can be rotated with a 2-DOF gimbal that holds a carbon fiber rod with flexures and rollers to constrain the rod and other parts in terms of rotation while allowing linear actuation (Figure 3b). Details of the actuator design are provided in [22].

The gimbal handle constrains two linear actuators and allows 3-DOF free rotation of the user's hand. All rotational axes of the gimbal handle as well as linear actuator axes cross the center of rotation of the handle. Thus, only desired forces are delivered to the user's hand and there is no residual torque. The gimbal handle allows only small structural deflections, as the size of the handle is small compared to the range of linear actuators. Deflection of the linear actuators is very small because only axial loads are applied via the gimbal. The axial stiffness of the linear actuator is dependent on the timing belt stiffness, which is usually very high and has a wide range of choices. Further, the parallel actuation mechanism enhances the overall stiffness at the end-effector. The end-effector ROM can be enlarged by increasing the span between the linear actuator gimbal and the linear motion range of the actuator. This does not compromise inertia or friction, as the available force is not changed by the ROM and both the timing belt and linear rod of the actuator have very little inertia. Thus, the system is scalable, unlike previously developed systems mentioned in Section 1, satisfies stiffness requirements, and affords a large ROM without significantly increasing the inertia. Table 1 lists the detailed specifications of the proposed haptic interface. The total linear inertia of moving parts, which include the rod, timing belt, and belt tensioner, is 0.533 kg. The gimbal handle linkages are manufactured using a 3D printer and the joints are composed of metal parts.

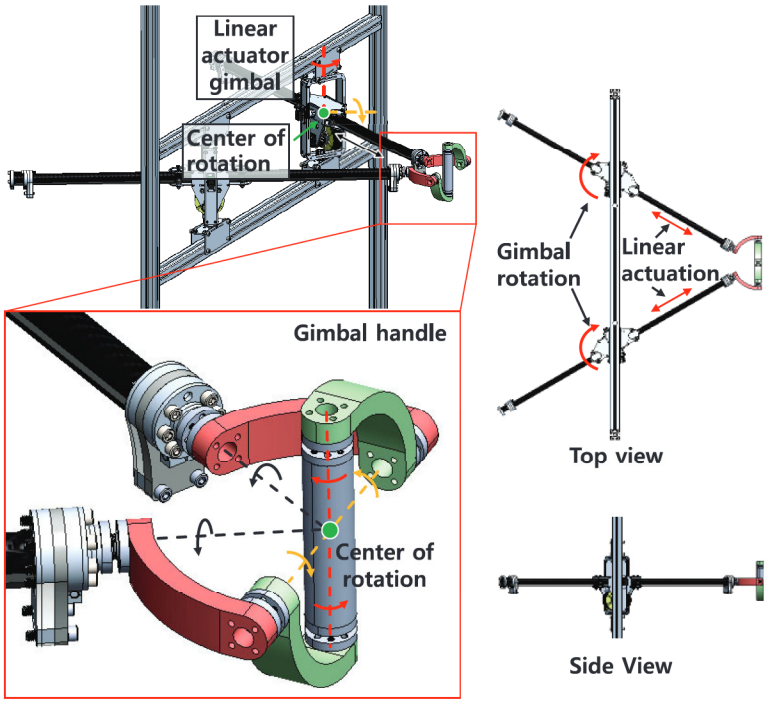

(**a**)

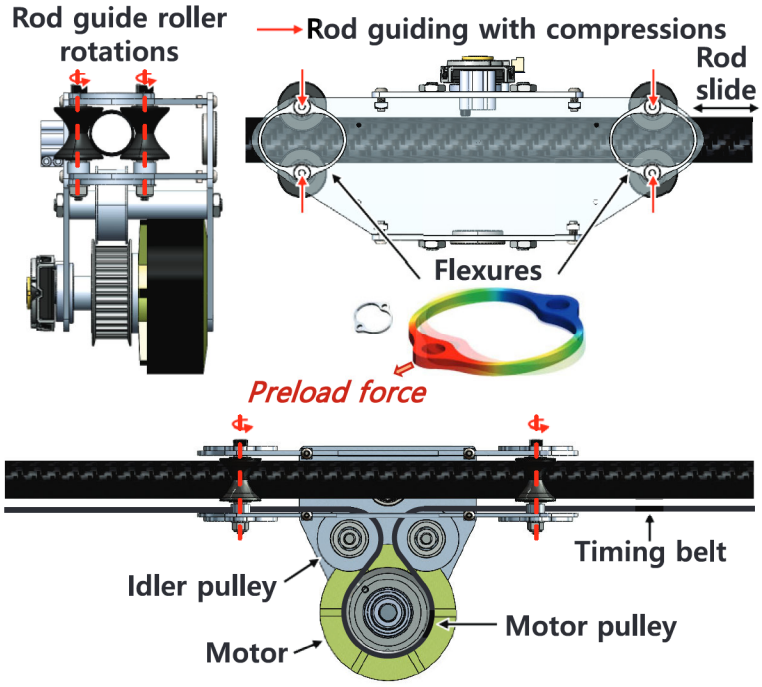

(**b**)

Figure 3. Detailed design of the proposed haptic interface: (**a**) overview of the system and (**b**) linear motion guidance mechanism of the actuator.

Table 1. Specifications of the 2-DOF haptic interface.

	Specification
Min. available force at home position	83 N (Continuous) 166 N (Peak)
Motor	Turnigy 9235–100 KV Pulley radius: 28.245 mm Nominal torque: 2.825 Nm
Sensor	Motor encoder: 14 bit incremental Actuator gimbal encoder: 12 bit absolute
Controller	NI cRIO-9082 Control rate: 1 kHz FPGA clock: 40 MHz
Linear motion rod	Material: CFRP OD: 25.4 mm ID: 22.86 mm Length: 1219 mm Weight: 158 g
Timing belt	Gates PowerGrip GT3 5MGT Glass fiber reinforced
Gimbal handle	Material: ABS and steel Weight: 562 g

The proposed haptic interface design can be expanded to devices with more DOFs and feedback forces/torques by changing the number of modular linear actuators and employing a suitable end-effector to connect the linear actuators. As an example, a 3 DOF *Agile Eye*-like [26] gimbal with three modular linear actuators could be applied (Figure 4). The advantage of the agile eye-like gimbal designs proposed here is the absence of residual torque even though the system has fewer DOFs than six. Stewart platform-type mechanisms [27] with six linear actuators and universal joints can be used if six DOFs are required. The actuator of a Stewart platform typically has high inertia and low backdrivability, as significant reduction is used with a focus on precise position control and stiffness. This limitation can be overcome by our linear actuator. However, this paper focuses on the evaluation of the manipulator. The comparative design of these kinds of handles, including those for other mechanisms, is not described in detail. In this paper, a 2-DOF prototype is analyzed for comparison with conventional mechanisms.

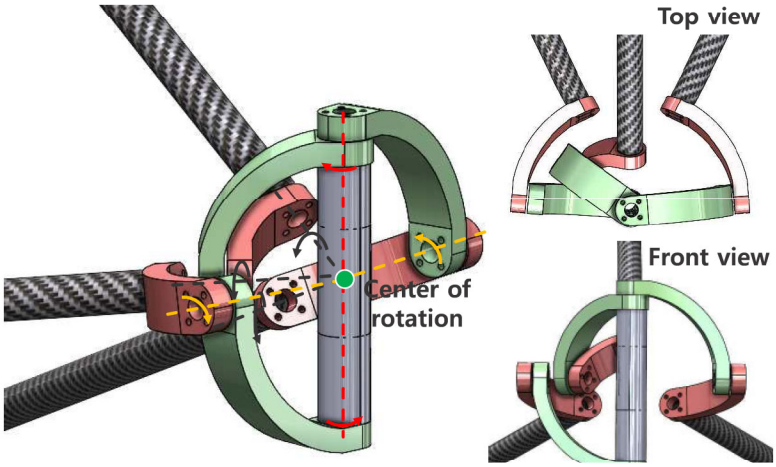

Figure 4. A 3-DOF handle design concept. All linear actuator axes and rotational axes of the gimbal cross the center of rotation.

2.2. Analysis

The advantages of the linear actuator-based haptic interface as compared to conventional rotational mechanisms are discussed next. The key metric is the reflected inertia, as the high-frequency performance of a haptic interface is dominated by inertia [15]. The force capability is important as well, as high force is a key requirement of many applications. Thus, we introduce the concept of ***Haptic Force Density*** (Figure 5), i.e., the force capability per unit of reflected inertia:

$$\boldsymbol{F_r}(\boldsymbol{q}, \theta_{F_r}) = \boldsymbol{u}\frac{|\boldsymbol{F}(\boldsymbol{q}, \theta_{F_r})|}{|\boldsymbol{I}(\boldsymbol{q}, \theta_{F_r})|}, \tag{1}$$

where $\boldsymbol{u}$ is the unit vector corresponding to the angle θ_{F_r}, $\boldsymbol{q}$ is the actuator displacement vector, and $\boldsymbol{F}(\boldsymbol{q}, \theta_{F_r})$ is the force that the device can generate at the end-effector in the quasi-static state, calculated as follows:

$$\boldsymbol{F}(\boldsymbol{q}, \theta_{F_r}) = \boldsymbol{J^{-T}}(\boldsymbol{q})\boldsymbol{\tau} \tag{2}$$

where $\boldsymbol{J}$ is the 2×2 Jacobian derived from the 2D end-effector position. The mechanism was modeled on a 2D plane aligned with the two linear actuator axes. $\boldsymbol{I}(\boldsymbol{q}, \theta_{F_r})$, which is the reflected inertia perceived by the user when the end-effector is back-driven with unit acceleration (1 m/s^2), is calculated as [28]:

$$\boldsymbol{I}(\boldsymbol{q}, \theta_{F_r}) = \boldsymbol{J^{-T}}(\boldsymbol{q})\boldsymbol{M}\boldsymbol{J^{-1}}(\boldsymbol{q})\ddot{\boldsymbol{x}} = \boldsymbol{\Lambda}(\boldsymbol{q})\ddot{\boldsymbol{x}} \tag{3}$$

Here, θ_{F_r} indicates the direction of the generated force, which corresponds to a set of actuator torques $\boldsymbol{\tau}$ or the direction of the back-driven task-space inertial force, while $\boldsymbol{M}$ is the inertia matrix determined by the actuator inertia and the system mechanism. The characteristics of the haptic force density $\boldsymbol{F_r}(\boldsymbol{q}, \theta_{F_r})$ are varied by the actuation mechanism, as $\boldsymbol{F_r}(\boldsymbol{q}, \theta_{F_r})$ is related to the Jacobian determined by the geometry of the device.

A higher $\boldsymbol{F_r}(\boldsymbol{q}, \theta_{F_r})$ indicates that the displayable force magnitude in a specific direction $\boldsymbol{u}$ that corresponds to the angle θ_{F_r} is larger compared to that of the reflected inertia when the haptic device is backdriven by the user in the same direction. A haptic device can render high forces with high haptic force density $\boldsymbol{F_r}(\boldsymbol{q}, \theta_{F_r})$ in comparison to its perceived (reflected) inertia, meaning that the user feels less inertial resistance at higher haptic force density at the same available force. This implies that the system is probably more transparent, as the inertia is small compared to the available force. Usually, haptic devices have $(\boldsymbol{a})$ negligible perceived inertia and can only generate small forces due to a small gearing ratio (<10:1), or $(\boldsymbol{b})$ can generate very high forces at the expense of very large passive reflected inertia by employing gearboxes with a large gearing ratio (>100:1). In either case, the haptic force density is small. In this paper, we focus on increasing the force capability without inflating the task space inertia of the device.

Figure 6 shows the force capability, reflected inertial force, and their ratio of a haptic interface with respect to (a) a parallel linear mechanism (this work), (b) a serial rotational mechanism, and (c) a parallel rotational mechanism. The motors are assumed to be at the bases, minimizing the inertia induced by the motor mass. The parallel linear mechanism represents the haptic interface mechanism proposed in this paper (Figure 6a), which has two passive rotational joints ($\theta_{1,l}$ and $\theta_{2,l}$) and two linear joints actuated by the motor ($l_{1,l}$ and $l_{2,l}$). Small rotational inertia is assumed because most of the mass (the motor and metal parts) are near the gimbal center. Thus, the linear actuator dynamics dominate the system, and are considered in the inertia matrix $\boldsymbol{M}$. The other two mechanisms are conventional haptic interface designs utilizing rotational actuation mechanisms. In a serial rotational mechanism [7–9], the first motor actuates the first joint, which corresponds to $\theta_{1,s}$, and the second motor is attached to the first link (Figure 6b). The second motor rotates the second joint ($\theta_{2,s}$) relative to the first linkage. In contrast, the motors of the parallel rotational mechanism are independent (Figure 6c). Both motors are fixed to the base and independently connected to the two joints. Thus, each joint motion depends only on

the motor motion corresponding to the joint. The parallel rotational mechanism can be considered as a linearized version of linkage-based mechanisms [10–13,20,21] under the assumption that the transmission through the second joint is rigid enough.

The link lengths of the rotational mechanisms were set to 600 mm each to cover the required ROM (600 mm × 600 mm), i.e., from the shoulder to the maximum arm extension, without significant singularity. The same motor as in our linear actuator-based haptic interface was assumed. The gear ratios were 21:1 and 18:1 for the serial and parallel rotational mechanisms, respectively. These ratios were selected to generate the same minimum force of the parallel linear mechanism at the home positions shown in the figure in order to ensure a fair comparison.

The blue lines in Figure 6 are the available force at each position in all directions ($\boldsymbol{F}(\boldsymbol{q}, \theta_{F_r})$), while the black ellipsoids denote the reflected inertia when the end-effectors are backdriven with unit acceleration ($\boldsymbol{I}(\boldsymbol{q}, \theta_{F_r})$). The haptic force density $\boldsymbol{F_r}(\boldsymbol{q}, \theta_{F_r})$ was calculated by dividing the force by inertia for all directions. As shown in the figure, the force and inertia characteristics differ depending on the mechanism. The parallel linear and rotational mechanisms show Cartesian coordinate-based characteristics, while the serial rotational mechanism has the characteristics of polar coordinates. The parallel mechanisms in Figure 6a,c exhibit more even force and inertia distributions than the serial mechanism, although visual comparison with separate figures is difficult.

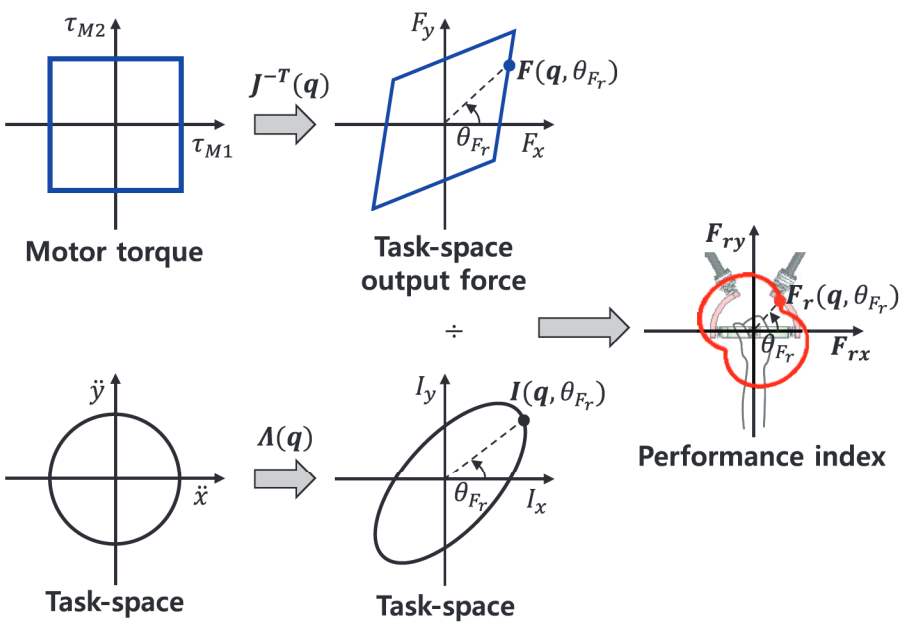

Figure 5. The concept of haptic force density $\boldsymbol{F_r}(\boldsymbol{q}, \theta_{F_r})$, provided by the device's force capability per unit of reflected inertia for a certain direction.

The haptic force density of the three mechanisms are overlapped in Figure 7 for easier comparison. The parallel linear mechanism usually has the largest haptic force density. The relative haptic force density of the parallel linear mechanism becomes higher along the y direction compared to those of other mechanisms. This is advantageous for a haptic interface that requires a wide ROM. The advantage of the proposed system is apparent when the minimum values of the haptic force density are compared. The minimum $\boldsymbol{F_r}(\boldsymbol{q}, \theta_{F_r})$ values are 0.875, 1.299, and 1.706 for the serial rotational, parallel rotational, and parallel linear mechanisms, respectively; this implies that the parallel linear mechanism provides a better haptic experience in terms of the force capability over the reflected inertia.

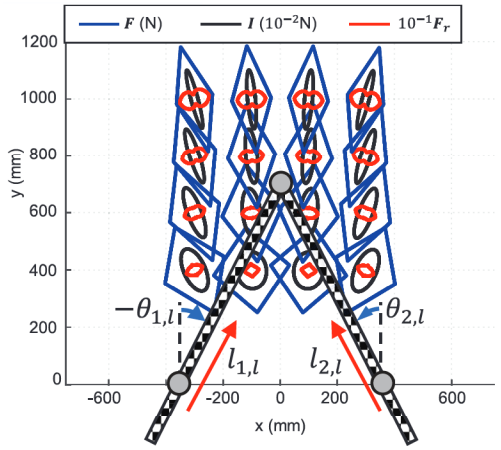

(**a**)

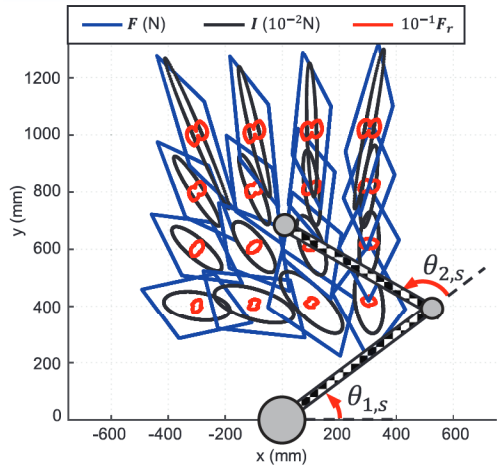

(**b**)

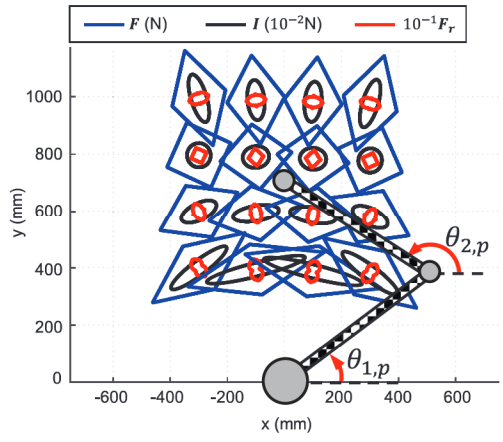

(**c**)

Figure 6. Force capability, inertial force, and their ratio for different haptic interface mechanisms: (**a**) the proposed parallel linear mechanism, (**b**) serial rotational mechanism, and (**c**) parallel rotational mechanism.